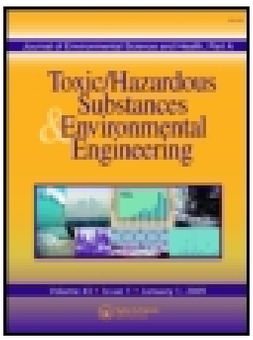

Taylor & Francis
Taylor & Francis Group

Journal of Environmental Science and Health, Part A
Toxic/Hazardous Substances and Environmental Engineering

ISSN: 1093-4529 (Print) 1532-4117 (Online) Journal homepage: http://www.tandfonline.com/loi/lesa20

Synthesis and performance evaluation of Al/Fe oxide coated diatomaceous earth in groundwater defluoridation: Towards fluorosis mitigation

Anthony A. Izuagie, Wilson M. Gitari & Jabulani R. Gumbo

To cite this article: Anthony A. Izuagie, Wilson M. Gitari & Jabulani R. Gumbo (2016): Synthesis and performance evaluation of Al/Fe oxide coated diatomaceous earth in groundwater defluoridation: Towards fluorosis mitigation, Journal of Environmental Science and Health, Part A, DOI: 10.1080/10934529.2016.1181445

To link to this article: http://dx.doi.org/10.1080/10934529.2016.1181445

Published online: 24 May 2016.

JOURNAL OF ENVIRONMENTAL SCIENCE AND HEALTH, PART A
2016, VOL. 0, NO. 0, 1–15
http://dx.doi.org/10.1080/10934529.2016.1181445

Taylor & Francis
Taylor & Francis Group

Synthesis and performance evaluation of Al/Fe oxide coated diatomaceous earth in groundwater defluoridation: Towards fluorosis mitigation

Anthony A. Izuagie[a,b], Wilson M. Gitari[a,b], and Jabulani R. Gumbo[c]

[a]Department of Ecology and Resource Management, University of Venda, Thohoyandou, South Africa; [b]Environmental Remediation and Pollution Chemistry Research Group, School of Environmental Sciences, University of Venda, Thohoyandou, South Africa; [c]Department of Hydrology and Water Resources, University of Venda, Thohoyandou, South Africa

ABSTRACT

The quest to reduce fluoride in groundwater to WHO acceptable limit of 1.5 mg/L to prevent diseases such as teeth mottling and skeletal fluorosis was the motivation for this study. Al/Fe oxide-modified diatomaceous earth was prepared and its defluoridation potential evaluated by batch method. The sorbent with pH_{pzc} 6.0 ± 0.2 is very reactive. The maximum 82.3% fluoride removal attained in 50 min using a dosage of 0.3 g/100 mL in 10 mg/L fluoride was almost attained within 5 min contact time; 81.3% being the percent fluoride removal at 5 min contact time. The sorbent has a usage advantage of not requiring solution pH adjustment before it can exhibit its fluoride removal potential. A substantial amount of fluoride (93.1%) was removed from solution when a sorbent dosage of 0.6 g/100 mL was contacted with 10 mg/L fluoride solution for 50 min at a mixing rate of 200 rpm. The optimum adsorption capacity of the adsorbent was 7.633 mg/g using a solution containing initially 100 mg/L fluoride. The equilibrium pH of the suspensions ranged between 6.77 and 8.26 for 10 and 100 mg/L fluoride solutions respectively. Contacting the sorbent at a dosage of 0.6 g/100 mL with field water containing 5.53 mg/L at 200 rpm for 50 min reduced the fluoride content to 0.928 mg/L—a value below the upper limit of WHO guideline of 1.5 mg/L fluoride in drinking water. The sorption data fitted to both Langmuir and Freundlich isotherms but better with the former. The sorption data obeyed only the pseudo-second-order kinetic, which implies that fluoride was chemisorbed.

ARTICLE HISTORY
Received 4 November 2015

KEYWORDS
Defluoridation; diatomaceous earth; fluorosis; groundwater; mitigation; synthesis

Introduction

In rural Africa and Asia, groundwater remains the most appropriate drinking water where there is lack of pipe-born water. This is essentially because it is usually free from microbial contamination commonly associated with surface water and also less prone to effluent from industries. However, groundwater may not be completely safe for consumption if the fluoride level is above WHO guideline of 1.5 mg/L in drinking water.[1] Far above any other contributory source, high fluoride in drinking water is traced to leaching of fluoride from fluoride-containing minerals such as fluorspar, cryolite and fluorapatite.[2] Fluoride is necessary in drinking water in appropriate concentration (0.5–1.0 mg/L) to prevent dental caries in children.[3] Where drinking water contains fluoride above 1.5 mg/L, there is an increasing risk of dental fluorosis, and much higher concentrations lead to skeletal fluorosis.[4]

Several defluoridation methods have been employed to remove excess fluoride from drinking water. These methods could be classified as adsorption, ion-exchange, precipitation/coagulation, electrocoagulation and membrane processes.[5–7] Research in adsorption technology for fluoride removal has been far more embraced than any other technology. Defluoridation based on adsorption technology is considered to be the most appropriate for rural communities because of its low cost, ease of operation, needless of operational skill and electric power to run. In the light of these factors, some of the materials that have been tested include activated charcoal,[8] activated alumina,[9] clay soils and their modified species [10,11] and aluminium hydroxide impregnated macroreticular aromatic polymeric resin [12] among others.

Raw diatomaceous earth (DE) has a low fluoride removal potential. The highest percent fluoride removal at optimum adsorption conditions is between 23.4% and 25.6% for 8 mg/L fluoride at pH 2, contact time of 30 min, solid-liquid ratio of 0.4 g/50 mL, and shaking speed of 200 rpm. The use of raw DE for fluoride removal from drinking water is further limited by the fact that it exhibits its fluoride removal characteristics at a very low pH. This limitation compels surface modification of DE, such that the application of the modified species in drinking water will not require pH adjustment. DE has pores which can be coated with metal hydroxides/oxides having high affinity for fluoride through precipitation from their salts. Metal oxides-modified DE has been employed in the removal of various contaminants such as heavy metals and dyes from textile effluent and wastewater.[13,14] DE is nonorganic and so cannot undergo degradation to foul water. Another advantage for using DE as a support material is its stability at the operating temperature. It is reported that the pore

CONTACT Anthony A. Izuagie aaizuagie@gmail.com Department of Ecology and Resource Management, University of Venda, Thohoyandou 0950, South Africa.
Color versions of one or more of the figures in this article can be found online at www.tandfonline.com/lesa.

structure of DE starts to collapse at 900°C. Also, complete dehydration of the material occurs from 900 to 1,200°C.[15]

Materials and methods

Sample preparation

A mass of 140 g of dry and clean pulverized DE was dispersed into 500 mL of Milli-Q water (18.2 MΩ cm at 25°C) in 1-L plastic bottle. The pH of mixture was adjusted to 11 using 0.1 M NaOH solution. The bottle was corked and shaken on a reciprocating shaker at 200 rpm for 30 min to remove geological fluoride. After equilibration, the mixture was centrifuged and the solid recovered was scooped into 1-L bottle containing some Milli-Q water. The mixture was acidified to pH 2 using 0.1 M HCl, shaken for 30 min and centrifuged. The solid was washed with Milli-Q water with repeated centrifuging until the pH of the supernatant was 6. The DE was dried in the oven at 110°C for 8 h, cooled in the desiccator and then stored in corked plastic bottles for future use.

Evaluation of fluoride released from diatomaceous earth

To ensure that the HCl- and NaOH-treated DE was free of geological fluoride, 0.4 g of the dry sample was dispersed into 40 mL of Milli-Q water followed by pH adjustment to 2 with 0.1 M HCl. The final volume of solution was made up to 50 mL by adding more Milli-Q water. The mixture was equilibrated at 200 rpm for 30 min. After equilibration, the mixture was centrifuged at 5,000 rpm for 5 min and the supernatant was analyzed for fluoride using four-standard calibrated ORION VERSASTAR Advanced Electrochemistry meter fluoride ion-selective electrode (LABOTEC (PTY) LTD, South Africa). TISAB III was added to the standards and supernatant at volume ratio 1:10, allowed to stand for 40 min to ensure complete decomplexation of possible Al- or Fe-fluoride complexes, maintain a constant total ionic strength and adjust the pH to around 5.3 before fluoride measurement. (All subsequent cases of fluoride determination followed this procedure). The concentration of fluoride in the supernatant was 0.0016 mg/L as opposed to the value of 1.22 mg/L obtained when 0.4 g of non-treated DE was equilibrated under the same conditions.

Preparation of solutions

All the chemicals used, which included hydrochloric acid (HCl), sodium hydroxide (NaOH), sodium fluoride (NaF), iron (II) chloride tetrahydrate ($FeCl_2.4H_2O$), iron(III) tetraoxosulphate(VI) hydrate ($Fe_2(SO_4)_3.xH_2O$) and aluminium tetraoxosulphate(VI) octadecahydrate ($Al_2(SO_4)_3.18H_2O$) for the preparation of required solutions were of analytical grade. Chemicals were produced by Sigma-Aldrich, Germany and supplied by Rochelle Chemicals, South Africa.

A stock solution of 1,000 mL of 1,000 mg/L fluoride was prepared by dissolving 2.210 g of NaF in Milli-Q water in a litre volumetric flask. Lower concentrations of fluoride were prepared from the stock solution by serial dilution.

Computation equations

The percent fluoride removal was calculated using the following equation:

$$\%\ F^- \text{ removal} = \frac{(C_0 - C_e)}{C_0} \times 100. \quad (1)$$

C_0 and C_e are the initial and equilibrium concentrations of fluoride solution, respectively, in mg/L.

The adsorption capacity, q_e was computed using the following equation:

$$\text{Adsorption capacity} = \frac{(C_0 - C_e)}{m} \times V. \quad (2)$$

m is the mass of adsorbent in g, while V is the volume of fluoride solution in L.

Results and discussion

Al_2O_3- and Fe_2O_3-modifications of diatomaceous earth at optimum conditions

DE was modified separately with Al_2O_3 and Fe_2O_3. The effects of shaking speed and contact time on the two modifications were studied to evaluate the optimum conditions for the modification of diatomaceous with the metal oxides.

Effect of shaking speed

A mass of 2 g each of DE was dispersed into four 250-mL plastic bottles containing 20 mL of 0.5 M Al^{3+} solution and another four containing 20 mL of 0.5 M Fe^{2+} solution. The bottles were corked and shaken on a Stuart reciprocating shaker at 200 rpm for 20 min to ensure thorough soaking. After shaking, 20 mL of 2 M NaOH was measured into the bottles to precipitate Al $(OH)_3$ and $Fe(OH)_2$. Mixtures were shaken, respectively, at 100, 150, 200 and 250 rpm for 30 min to evaluate the effect of shaking speed on the modification of DE with Al_2O_3 and Fe_2O_3. The various mixtures were centrifuged after equilibration. The supernatants from $Al(OH)_3$-DE-NaOH mixture were discarded while those from $Fe(OH)_2$-DE-NaOH mixtures were acidified and kept for analysis with inductively coupled plasma-mass spectrometry (ICP-MS). All the solids from $Al(OH)_3$-DE-NaOH mixtures were washed with 100 mL of Milli-Q water and dried in the oven at 110°C for 8 h, cooled in the desiccator and stored in corked plastic bottles. The solids from $Fe(OH)_2$-DE-NaOH mixtures were left exposed to air for 10 h for oxidation of Fe^{2+} to Fe^{3+}. At oxidation, the green colour of the solids turned completely brown; evidence of oxidation of Fe^{2+} to Fe^{3+}. The solids were later washed as in the case of solids from $Al(OH)_3$-DE-NaOH mixtures and dried in the oven at 110°C for 8 h.

Aliquots of 10 mL of the supernatants from the $Fe(OH)_2$-DE-NaOH mixtures were acidified with 2 mL of 3 M HNO_3 for ICP-MS analysis. A blank for the analysis was prepared following the same procedure as the samples. The acidified supernatants and the blank were analyzed for Fe. The results of analyses are reported in Table 1. The least concentration of Fe in solution implies highest coating with Fe_2O_3. Hence, the

Table 1. Concentrations of Al_2O_3 and Fe_2O_3 in solutions at different shaking speeds.

Shaking speed in rpm	Concentration of dissolved Al^{3+} (mg/L)	Concentration of Al^{3+} from DE (mg/g)	Concentration of Fe species in supernatant (mg/L)
100	197.61	49.40	0.90
150	153.49	38.37	1.20
200	124.30	31.07	0.84
250	107.90	26.97	2.16

shaking speed of 200 rpm was the optimum speed for DE modification with Fe_2O_3 as shown in the table. Dissolution of Al from Al_2O_3-modified DE samples was used to evaluate the effect of shaking speed on modification with Al_2O_3. The procedure involved weighing 0.2 g of each Al_2O_3-modified DE sample and raw DE (blank) into 250-mL plastic bottles containing 50 mL of 3 M HNO_3. The bottles were tightly corked and the mixtures heated at 60°C for 2 h to dissolve Al_2O_3. After heating, the mixtures were cooled to room temperature and then filtered using membrane filters. The Al^{3+} in filtrates was determined using ICP-MS analysis. The results of analyses after blank correction are presented in Table 1. The highest value of Al^{3+} determined in solution implies the highest coating of DE with Al_2O_3. The corresponding shaking speed of 100 rpm was therefore the optimum shaking speed for modification with Al_2O_3.

Effect of contact time

The effect of contact time on DE modification with Al_2O_3 and Fe_2O_3 was considered following the procedure explained previously. However, the $Al_2(SO_4)_3$-DE-NaOH and $FeCl_2$-DE-NaOH mixtures in the 250-mL bottles were equilibrated at 200 rpm for 10, 20, 30, 40, 50 and 60 min. The supernatants from $Al(OH)_3$-DE-NaOH mixtures were discarded as the dry solids were to be treated for metal analysis while the supernatants from $Fe(OH)_2$-DE-NaOH were acidified for ICP-MS analyses as described in the previous subsection.

The results of the Al^{3+} and Fe^{3+} species analyses are reported in Table 2. As shown in this table, the optimum contact times were 50 and 60 min, respectively, for DE modification with Fe_2O_3 and Al_2O_3.

Binary Al/Fe oxide modification of diatomaceous earth

Aliquots of 0.5 M Al^{3+} and 0.5 M Fe^{2+} solutions were added together at different proportions in 250-mL plastic bottles with the final volume of each resulting solution being 20 mL. The volume ratios of Al^{3+} to Fe^{2+} considered were 2.5:17.5, 5:15, 10:10, 15:5 and 17.5:2.5, subsequently represented as AF-D1, AF-D2, AF-D3, AF-D4 and AF-D5, respectively. A mass of 2 g each of DE was weighed into each of the bottles and shaken for 20 min at 200 rpm to ensure proper soaking of DE. An aliquot of 20 mL of 2 M NaOH was transferred into each of the bottles to precipitate $Al(OH)_3$ and $Fe(OH)_2$. The mixtures were shaken for 50 min at 100 rpm. After equilibration, the mixtures were centrifuged to remove excess NaOH solution. The solids were left exposed to air for 10 h for the oxidation of Fe^{2+} to Fe^{3+}. Thereafter, the solids were washed with 100 mL of Milli-Q water each, and centrifuged to remove the supernatants. The washed, binary metal hydroxide-DE mixtures were placed in the oven and dried at 110°C for 8 h. The dry samples were cooled in a desiccator; the dry lumps were crushed and passed through a 250-μm pore test sieve.

Aliquots of 40 mL of 10 mg/L fluoride solution were measured into five 250-mL plastic bottles. A mass of 0.4 g of each Al/Fe oxide-modified DE sample was weighed into the bottles and the pH of mixtures adjusted to 7 by adding 0.1 M HCl solution. The final volume of solution was made up to 50 mL by adding Milli-Q water thereby making the initial fluoride concentration to be 8 mg/L. The mixtures in the bottles were shaken inside a thermostated water bath for 30 min at 200 rpm and 298 K. After equilibration, the mixtures were centrifuged and the supernatants analyzed for residual fluoride. The results are presented in Table 3.

The optimum defluoridation was obtained with AF-D3 which contained Al and Fe in the same proportion.

Comparison of the defluoridation potentials of Al_2O_3-, Fe_2O_3- and Al/Fe oxide-modified diatomaceous earth

The process of leaving $Fe(OH)_2$-DE-NaOH solids for hours to accomplish oxidation of Fe^{2+} to Fe^{3+} led to much loss of DE which being an amorphous silica is soluble at high pH. To avoid the problem of loss of material, Fe^{3+} salt was used in subsequent modifications requiring Fe^{3+} in the composite. With the use of Fe^{3+} salt, no further oxidation of metal was required. Therefore, $Fe_2(SO_4)_3.\times H_2O$ was used in place of $FeCl_2.4H_2O$.

The defluoridation potentials of single metal oxide-, Al_2O_3- and Fe_2O_3-modified DE were compared with that of the binary Al/Fe oxide-modified DE. The modified DE species were represented by ADE, FDE and AFDE, respectively.

AFDE was prepared by mixing 10 mL of 0.5 M Al^{3+} and 10 mL of 0.5 M Fe^{3+} solutions together in a 250-mL flask and then adding 2 g of DE. The mixture was swirled for about 1 min and left to stand for 2 h for DE to be properly soaked in solution. $Al(OH)_3$ and $Fe(OH)_3$ were co-precipitated on DE by

Table 2. Concentrations of Al_2O_3 and Fe_2O_3 in solutions at different contact times.

Contact time (min)	Concentration of dissolved Al^{3+} (mg/L)	Concentration of Al^{3+} from DE (mg/g)	Concentration of residual Fe species in supernatant (mg/L)
10	121.40	30.35	1.28
20	115.20	28.80	1.24
30	124.30	31.07	1.15
40	114.70	28.67	1.16
50	119.70	29.92	1.02
60	137.90	34.47	1.20

Table 3. Percent fluoride removal by Al/Fe oxide-modified DE containing different metal ratios.

Sample of Al/Fe oxide-modified DE	pH_e	C_e (mg/L)	% fluoride removal
AF-D1	7.26	6.74	15.8
AF-D2	7.31	5.52	31.0
AF-D3	7.26	4.69	41.4
AF-D4	7.31	4.94	38.3
AF-D5	7.25	5.61	29.9

Table 4. Percent fluoride removal using different metal oxide-modified DE samples.

Modified DE	pH_0	pH_e	C_e (mg/L)	% F^- removal
ADE	6.90	6.56	0.345	96.6
FDE	6.55	6.50	6.28	37.2
AFDE	6.51	6.43	0.302	97.0

adjustment of pH to 8.2 with addition of 2 M NaOH. The mixture was stirred vigorously as NaOH was being added. The same procedure was adopted for precipitation of $Al(OH)_3$ in a mixture of 20 mL of 0.5 M Al^{3+} and 2 g of DE, as well as $Fe(OH)_3$ in a mixture 20 mL of 0.5 M Fe^{3+} and 2 g of DE. The modification mixtures were shaken on a reciprocating shaker at 100 rpm for 50 min bearing in mind the limiting shaking speed and contact time for modification of DE with Al_2O_3 and Fe_2O_3 as explained earlier. The mixtures were centrifuged to remove excess NaOH while each solid was washed with 100 mL of Milli-Q water accompanied with centrifuging. The solids were dried in the oven at 110°C for 8 h, cooled in a desiccator and stored in corked plastic bottles to avoid moisture.

To evaluate the defluoridation potential of the modified DE species, 0.4 g of each sample was weighed into 50-mL aliquots of 10 mg/L fluoride solution in three 250-mL plastic bottles. The initial pH of each mixture was measured. The bottles were corked and shaken for 30 min. The equilibration pH was determined at the end of the equilibration time. The mixtures were then centrifuged and the clear supernatants obtained were analyzed for residual fluoride. The results of the percent fluoride removal are reported in Table 4.

As shown in Table 4, AFDE (Al/Fe oxide-modified DE) had the highest defluoridation potential (97.0% fluoride removal) of the three modified DE species and closely followed by ADE (96.6% fluoride removal). FDE had the least defluoridation potential. No pH adjustment of mixtures was effected since this would not be necessary in the application of adsorbents for defluoridation of drinking water in point-of-use systems.

Physicochemical characterization of Al/Fe oxide-modified diatomaceous earth

Surface area analysis

The surface area, pore area and volume of Al/Fe oxide-modified DE were analyzed at the National Centre for Nano-Structured materials, Council for Scientific and Industrial Research (CSIR), South Africa using the Brunauer–Emmett–Teller (BET) method. The instrument for analysis was Micromeritics TriStar II *Surface Area and porosity*. The results of analysis are compared with those of the raw DE as reported in Table 5.

The BET surface area increased from 31.9 m^2/g (raw DE) to 70.7 m^2/g (Al/Fe oxide-modified DE). Khraisheh et al.[14] reported a surface area of 80 m^2/g for manganese oxides modified DE while a value of 81.8 m^2/g was reported for aluminium compounds modified DE by Datsko et al.[16] The use of 2 M aluminium sulphate solution by Datsko et al.[16] for DE modification as against 0.25 M of Al^{3+} and 0.25 M Fe^{3+} solutions used in the study is an indication that the specific surface area of metal oxide-modified DE could vary much with the concentration of solution of metal salts. As shown in Table 5, increase in the surface area of DE after modification is evidence that Al/Fe oxide was deposited on the raw DE. Increase in surface area of adsorbent implies an increase in the number of active adsorption sites. There was a corresponding increase in pore volume of the adsorbent. The increase in pore surface area and volume is an indication that the percolation of water through the pores of the adsorbent during defluoridation would be more readily achieved.

The plot of pore volume against pore diameter for both raw and Al/Fe oxide-modified DE is shown in Figure 1. About 88% of the pores had their diameter within the pore diameter range of 2–50 nm (the mesopores range). Hence, the raw and Al/Fe oxide-modified DE are mesoporous materials. This fact shows that the adsorbent would be very permeable to water during defluoridation.

Morphological analysis of raw and Al/Fe oxide-modified diatomaceous earth

The morphology of the modified DE was probed by scanning with the Hitachi X-650 scanning electron micro analyser equipped with CDU lead detector at 25 kV. The scanning was carried out at the Electron Microscope Unit, University of Cape Town, South Africa. The images of the scans are presented in Figure 2. The images show the differences in the pores sizes and appearance of DE before and after modification. The pores of the modified DE appeared almost completely filled by Al/Fe oxide deposited on the pores of DE as opposed to the clear, net-like pores in the raw DE. The near closure of the pores of the modified DE is evidence that the raw DE was modified.

Fourier transform infra-red (FTIR) spectroscopy

The FTIR spectroscopic analyses of both modified DE and fluoride-treated modified DE were done using ALPHA FT-IR Spectrophotomer, to evaluate likely changes in the functional groups of the material on contact with fluoride solution. As shown in Figure 3, there was an increase in the transmittance of the Si-O-H stretching vibration at 454 cm^{-1} for the fluoride-treated DE. This could be possible because of the formation of Si-F bonds with fluoride adsorption which reduced the number of Si-O-H bonds on the adsorbent surface. The same trend was noticed for the transmittance at 1,059 cm^{-1} for Si-O-Si stretching vibration where possible replacement of some –O-Si bonds with F- could have occurred resulting in reduction of absorbance of IR by Si-O-Si.

Table 5. Comparison of the surface area, and pore area and volume of the raw and Al/Fe oxide-modified diatomaceous earth.

Form of diatomaceous earth (DE)	Single point surf. area (m^2/g)	BET surf. area (m^2/g)	BJH adsorption cum. surf. area of pores (m^2/g)	BJH desorption cum. surf. area of pores (m^2/g)	BJH adsorption cum. vol. of pores (cm^3/g)
Raw DE	31.1740	31.8861	21.405	22.6989	0.089054
Al/Fe oxide-modified DE	67.7887	70.7252	61.306	64.7792	0.121841

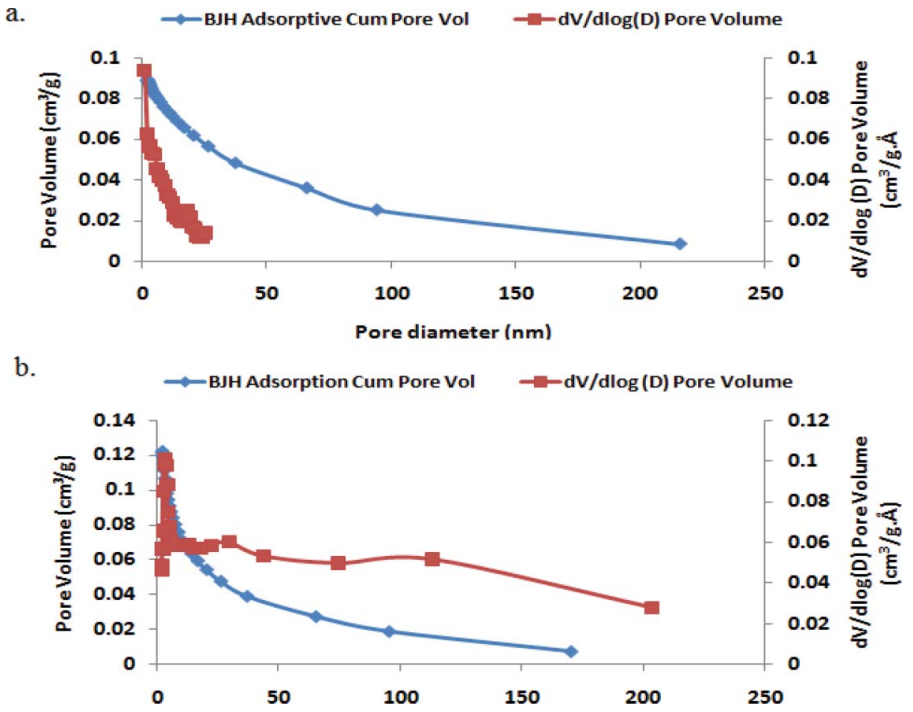

Figure 1. (a) Plot of BJH adsorption pore volume and BJH dV/dlog(D) pore volume against pore diameter (D) for raw DE. (b) Plot of BJH adsorption pore volume and BJH dV/dlog(D) pore volume against pore diameter (D) for Al/Fe oxide-modified DE.

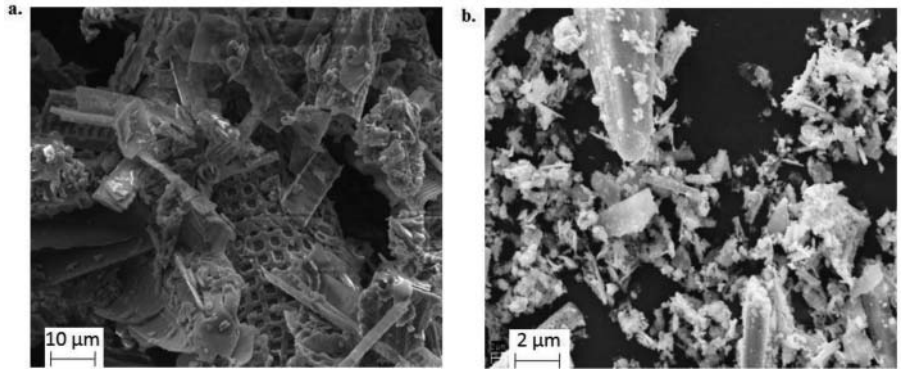

Figure 2. (a) SEM image of raw DE. (b) SEM image of Al/Fe oxide-modified DE.

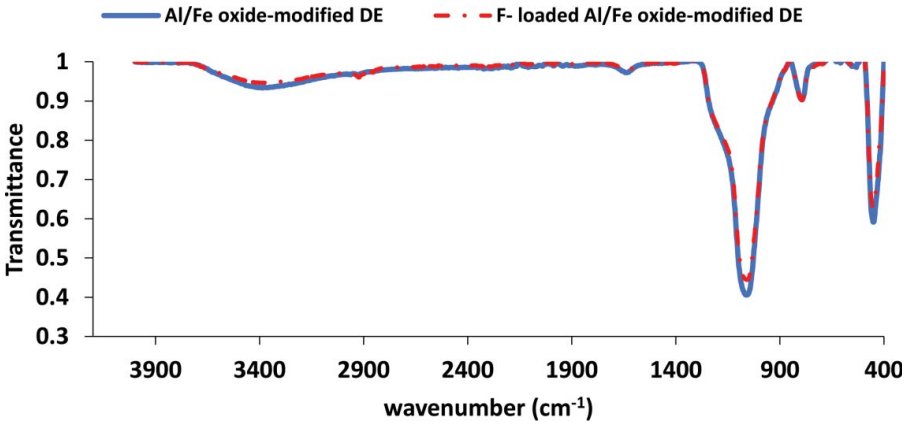

Figure 3. FTIR spectra of Al/Fe oxide-modified and F–loaded Al/Fe oxide-modified diatomaceous earth.

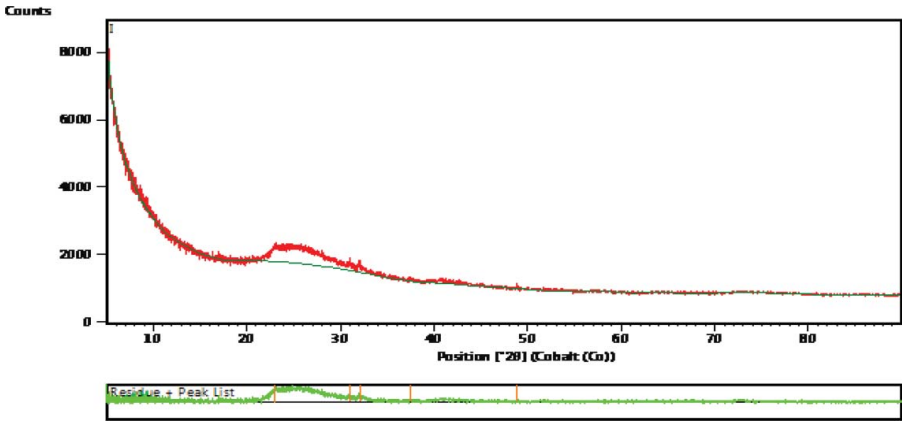

Figure 4. X-ray diffractogram of Al/Fe oxide-modified diatomaceous earth.

Thus, the modified DE removed fluoride on contact with fluoride solution.

X-ray fluorescence (XRF) analysis

The major elements in the raw and Al/Fe oxide-modified DE were analysed using PANalytical equipped with Rh tube. The analysis carried out at the ICP-MS & XRF Laboratory, Central Analytical Facilities, Stellenbosch University, South Africa are reported in terms of their percentage compositions. For the two materials, substantial difference in values was observed in the percentages of Al_2O_3, Fe_2O_3 and SiO_2 (Table 6). While there was an increase in the percent compositions of Al_2O_3 and Fe_2O_3 in the modified DE, the value of SiO_2 decreased. The increase in the values of the two metal oxides indicates the effective modification of DE.

X-ray diffraction (XRD) analysis

The X-ray diffraction analysis of Al/Fe oxide-modified DE was carried out at the XRD & XRF Facility, Faculty of Natural & Agricultural Sciences, Department of Geology, University of Pretoria, South Africa using PANalyticalX'Pert Pro powder diffractometer with X'Celerator detector and variable divergence and fixed receiving slits with Fe filtered Co-Kα radiation. The phases were identified using X'PertHighscore plus software. The X-ray diffractogram (Fig. 4) of Al/Fe oxide-modified DE shows that the material is completely amorphous. The peaks which are characteristics of crystalline materials are not visible. Hence, the modified DE had no crystalline mineral phase.

pH at point-of-zero charge (pH_{pzc})

The pH at point-of-zero charge of the prepared Al/Fe oxide-modified DE was evaluated using 1, 0.1 and 0.01 M KCl solutions. For a start, 60 mL of each solution were measured and the pH adjusted to a desired value with 0.1 M HCl and 0.1 M NaOH. The adjusted pH constituted the initial pH (pH_0). Aliquots of 50 mL of solutions of known pH were then measured into clean and dry 100-mL plastic bottles. A mass of 0.5 g of adsorbent was weighed into each bottle, corked and shaken inside a reciprocating waterbath shaker at 200 rpm for 24 h. The equilibrium pH (pH_e) of mixtures was determined as soon as the equilibration ended. The change in pH ($\Delta pH = pH_e - pH_0$) was plotted against the initial pH of KCl solution. The profiles of the plots for the adsorbent in the solutions of three KCl concentrations are presented in Figure 5. In the plots, the pH_{pzc} is the abscissa for $\Delta pH = 0$. This is the point where the curve crosses the horizontal axis.

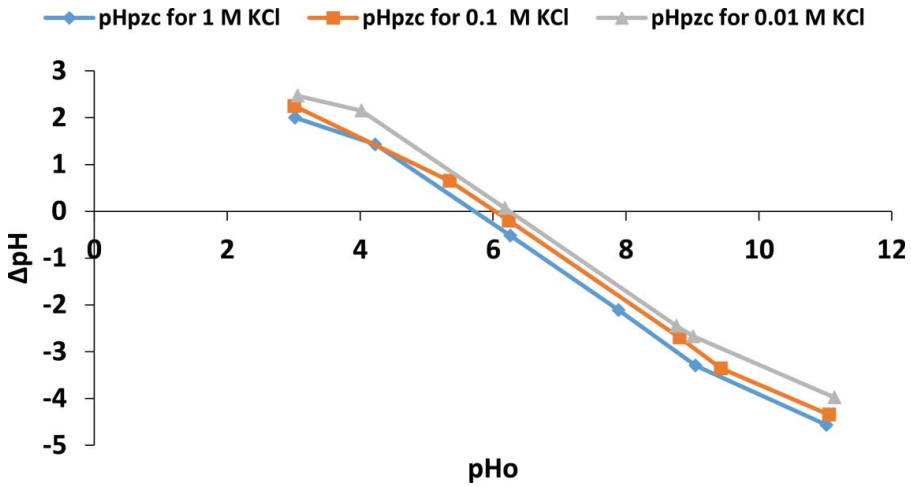

Figure 5. Determination of pH at point-of-zero charge of Al/Fe oxide-modified DE for 1, 0.1 and 0.01 M KCl (volume of solution: 50 mL, adsorbent dosage: 0.5 g, contact time: 24 h and shaking speed: 200 rpm).

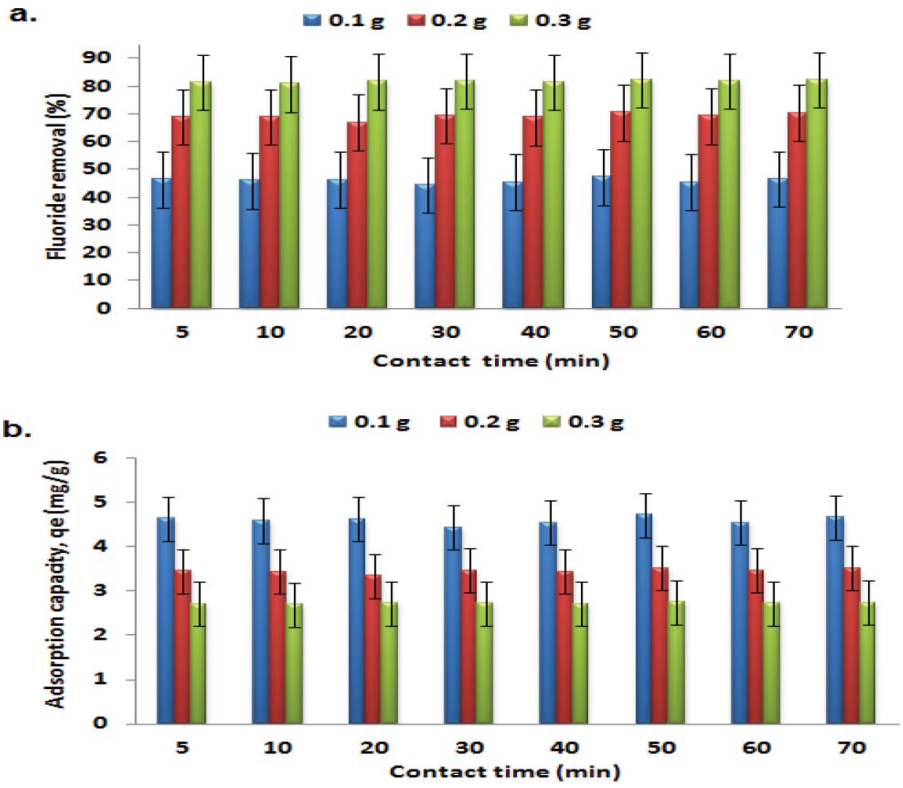

Figure 6. (a) Variation of percent fluoride removal with contact time. (b) Variation of adsorption capacity with contact time (initial fluoride concentration: 10 mg/L, volume of solution: 100 mL, and temperature: 297 K and shaking speed: 200 rpm).

From Figure 5, the values of pHpzc for 1, 0.1 and 0.01 M KCl were 5.75, 6.00 and 6.25 respectively. Therefore, the pHpzc of Al/Fe oxide-modified DE was 6.0 ± 0.2.

Optimization of adsorption conditions

Effect of contact time

Each 0.1 g of adsorbent was dispersed into 100 mL of 10 mg/L fluoride solution in eight 250-mL plastic bottles. The initial pH of suspensions was determined with a pH meter. The bottles were corked and shaken for 5, 10, 20, 30, 40, 50, 60 and 70 min at 200 rpm and 297 K. After equilibration, the equilibrium pH of each mixture was measured. The suspensions were centrifuged and the supernatants analyzed for fluoride as described previously. The batch experiment was repeated for adsorbent dosages of 0.2 and 0.3 g respectively. The results of analyses are reported in Figure 6. The residual fluoride was observed to be nearly constant at the evaluated contact times. This shows that the fluoride adsorption-desorption process attained equilibrium rapidly. Hence, no increase in contact time resulted in appreciable incremental fluoride removal. In the first 5 min, most of fluoride ions were adsorbed. A similar trend in fluoride removal was reported by Yao et al.[17] with the use of neodymium-modified chitosan for defluoridation of water. The mean difference between the percent fluoride removal at 5 and 50 min contact times at the evaluated dosages was approximately 1%.

Effect of adsorbent dosage

Adsorbent dosages of 0.1, 0.2, 0.4, 0.6, 0.8 and 1 g were weighed into 100 mL of 10 mg/L fluoride solution in six 250-mL plastic bottles. The mixtures were equilibrated at the optimum contact time of 50 min. Centrifugation of mixtures and fluoride analyses of supernatants were done as explained previously. Figure 7 shows how the percent fluoride removal and adsorption capacity varied with adsorbent dosage. The percent fluoride removal increased significantly from 0.1 to 0.6 g showing that the number of active adsorption sites increased with increase in dosage. The observed increase in fluoride adsorption with increasing sorbent dosage is in line with most reported defluoridation experiments involving different sorbent dosages.[17–19] At dosage values beyond 0.6 g, there was no appreciable increase in the per cent fluoride removal as the fluoride in solution was almost completely removed at lower dosages. A dosage of 0.6 g was chosen to be the optimum adsorbent dosage although a slightly higher fluoride removal occurred at higher sorbent dosages. The choice of 0.6 g was to see how a

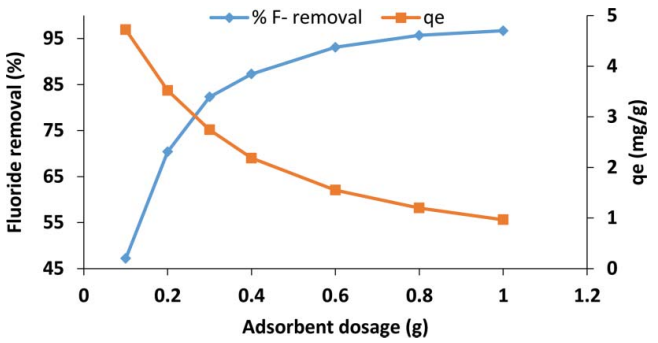

Figure 7. Variation of percent fluoride removal and adsorption capacity with adsorbent dosage (initial fluoride concentration: 10 mg/L, volume of solution: 100 mL, shaking speed: 200 rpm and temperature: 297 K).

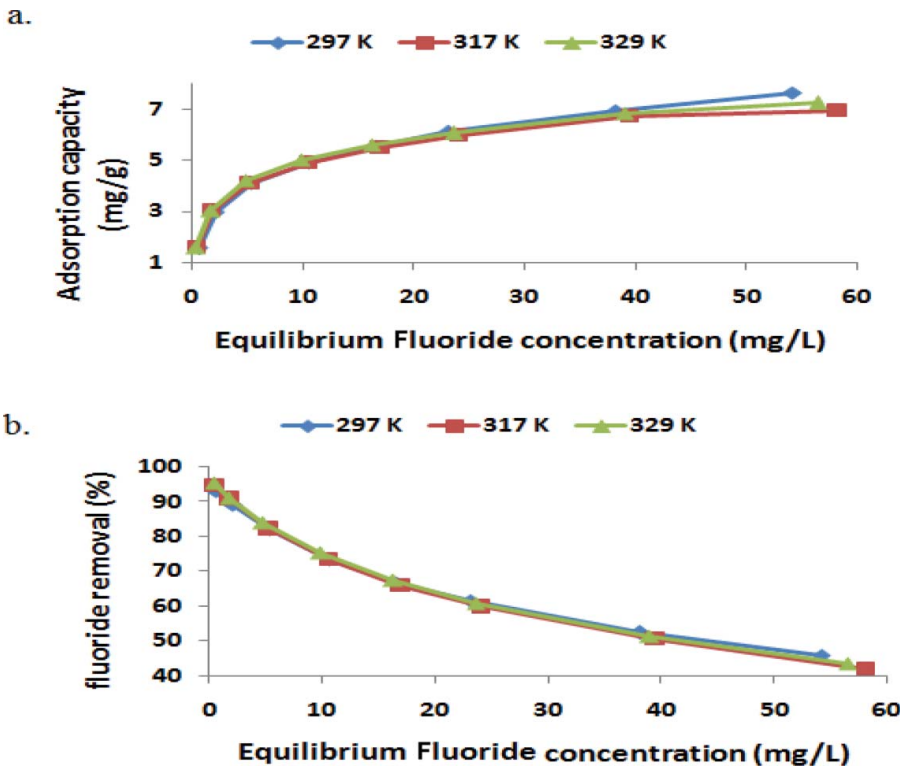

Figure 8. (a) Variation of adsorption capacity with adsorbate concentration. (b) Variation of percent fluoride removal with adsorbate concentration (initial fluoride concentration: 10 mg/L, volume of solution: 100 mL and shaking speed: 200 rpm).

relatively small dose of sorbent could ensure a good defluoridation of groundwater.

Effect of initial fluoride concentration

The effect of initial fluoride concentration was evaluated at 297, 317 and 329 K. In each batch experiment, 0.6 g of adsorbent was weighed into eight 250-mL plastic bottles containing 10, 20, 30, 40, 50, 60, 80 and 100 mg/L fluoride respectively and the mixtures equilibrated for 50 min. The initial and equilibrium pH of all the mixtures was measured. The fluoride in the supernatants was analyzed after centrifuging the mixtures.

The trends in the percent fluoride removal and the adsorption capacity with increasing equilibrium concentration at the evaluated temperatures are shown in Figure 8. The trends are consistent at the three temperatures. The percent fluoride removal decreased with increasing initial fluoride concentration.[20,21] This could have been because the mass of adsorbent was constant while there was an increase in the initial concentration of adsorbate. There would therefore be an increase in the equilibrium concentration of unadsorbed fluoride. However, the adsorption capacity of the sorbent increased rapidly as the initial concentration of fluoride increased from 10 to 30 mg/L after which there was a steady increase in the value until the initial concentration of 100 mg/L fluoride. The trend in the adsorption capacity with increasing initial fluoride concentration was as reported for various sorbents in literature.[21–23] The highest values of the adsorption capacity were 7.633, 6.967 and 7.250 mg/g at 297, 317 and 329 K respectively, for fluoride with an initial concentration of 100 mg/L. It was observed that the equilibrium pH increased with increasing initial fluoride concentration. This could be attributed to the fact that fluoride being highly electronegative could form hydrogen bond with water molecules with a net increase in the concentration of hydroxyl ions as the initial concentration of fluoride increased.

Effect of pH

It is widely reported that pH has an effect on adsorption of fluoride onto adsorbents.[23,24] Therefore, the effect of pH on fluoride sorption onto Al/Fe oxide-modified DE was evaluated. Aliquots of 90 mL of 12.5 mg/L fluoride were measured into six 250-mL plastic bottles. A mass of 0.6 g of adsorbent was then weighed into each bottle. The initial pH of mixtures was adjusted between 2 and 12 using 0.1 M HCl and 0.1 M NaOH. Milli-Q water was added to each bottle to top up the volume to 100 mL while noting the new pH on adding water. With the pH adjustment, the initial volume and fluoride concentration were 100 mL and 11.25 mg/L respectively. The bottles were corked and shaken for 50 min. After equilibration, the mixtures were centrifuged and the supernatants analyzed for residual fluoride. The values of percent fluoride removal and the corresponding adsorption capacity at various equilibrium pH values are reported in Figure 9.

As shown in Figure 9, the highest fluoride removal occurred at the equilibrium pH of 6.70. The least removal was observed at much higher pH values. Appreciable fluoride removal occurred within the pH range of 2.51–8.12.

The evaluated pH_{pzc} of Al/Fe oxide-modified DE was 6.0 ± 0.2. Below the pHpzc, the surface of adsorbent would be positively charged.[25] Above the pH_{pzc}, the adsorbent surface would be negatively charged. Fluoride removal above the pHpzc must have been by ion-exchange as OH- ions would predominate over H_3O^+ ions. This fact was corroborated by the results of the speciation calculations. Thus, the fluoride removal by ion-exchange occurred as

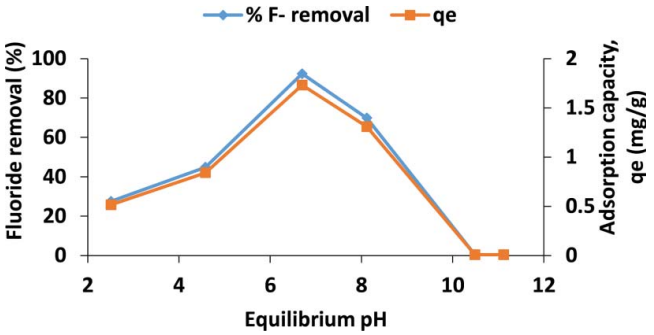

Figure 9. Variation of percent fluoride removal and adsorption capacity.

illustrated by the following equations:

$$Al(OH)_2^+ + 2F^- \rightarrow AlF_2^+ + 2OH^- \quad (3)$$

$$Al(OH)_3 + 3F^- \rightarrow AlF_3 + 3OH^- \quad (4)$$

$$Al(OH)_4^- + 4F^- \rightarrow AlF_4^- + 4OH^- \quad (5)$$

$$Fe(OH)_3 + 3F^- \rightarrow FeF_3 + 3OH^- \quad (6)$$

$$Fe(OH)_2^+ + 2F^- \rightarrow FeF_2^+ + 2OH^- \quad (7)$$

$$Fe(OH)_4^- + 4F^- \rightarrow FeF_4^- + 4OH^- \quad (8)$$

$$Fe(OH)^{2+} + F^- \rightarrow FeF^{2+} + OH^-. \quad (9)$$

The reduction in the per cent fluoride removal could be due to loss of large amount aluminium oxide at low pH. At pH <5, Al_2O_3 gets dissolved in an acidic medium causing a loss of adsorbent.[26,27] A number of factors could be attributed to the very low fluoride removal at alkaline pH. At pH >7, silicate and hydroxide compete more strongly with fluoride ions for exchange sites.[26,27] The colloidal brown colour (Fe^{3+} is brown) of the supernatants observed at pH >8 is evidence of loss of adsorbent at alkaline pH. DE, the main support for the coated binary metal oxide consists of amorphous silica which is very soluble at high pH. Also, Al_2O_3 is an amphoteric oxide which would react with OH- to form a soluble salt; leading to further loss of the adsorbent.

Effect of temperature

The effect of temperature on fluoride removal and adsorption capacity was evaluated at 297, 317 and 329 K using initial fluoride concentrations of 10, 20, 30, 40 50, 60, 80 and 100 mg/L. The experimental procedure was as described in the subsection where the effect of adsorbate concentration was explained. As shown in Figure 10, there was no significant change in the percent fluoride removal and adsorption capacity for each concentration of fluoride at the evaluated temperatures. This implies that change in temperature had no effect on the sorption process. The adsorbent would therefore be applicable for household defluoridation of groundwater at the ambient temperature. The negative values of the Gibbs free energy even at the least evaluated temperature reported in a later table is a confirmation of the feasibility of adsorption at that temperature.

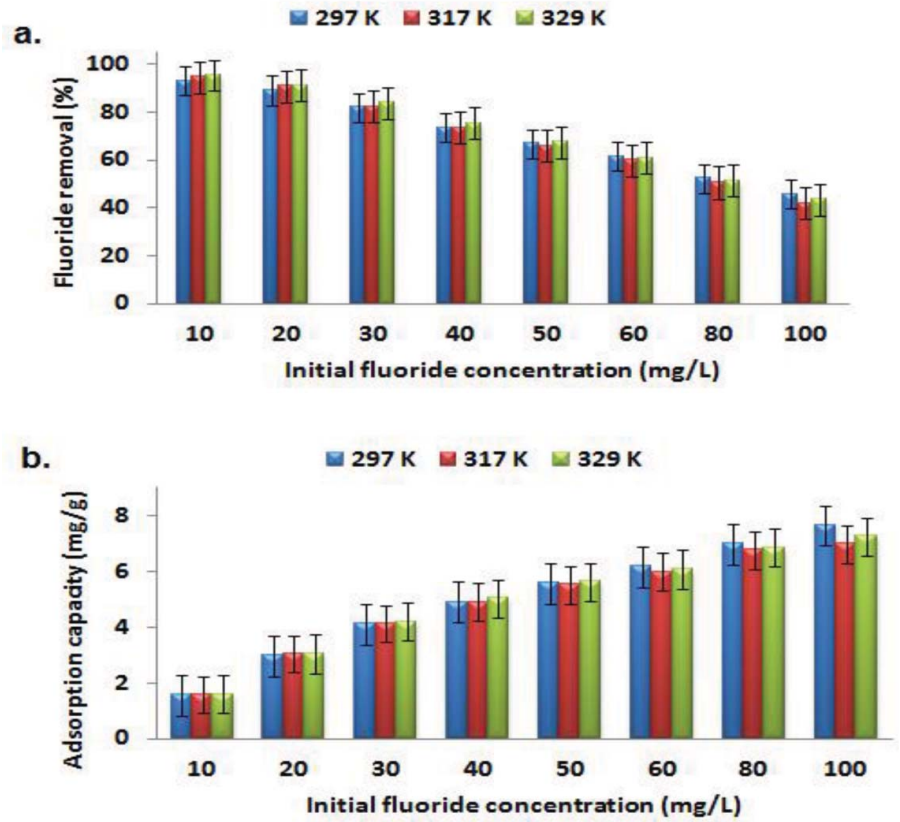

Figure 10. (a) Percent fluoride removal as a function of temperature. (b) Adsorption capacity as a function of temperature (contact time: 50 min, adsorbent dosage: 0.6 g/100 mL, temperature: 297, 317, and 329 K and shaking speed: 200 rpm).

Table 6. Major elements analysis by X-ray fluorescence.

Metal oxide	Raw diatomaceous earth	Al/Fe oxide modified diatomaceous earth
Al_2O_3	4.01	9.85
CaO	0.24	0.19
Cr_2O_3	0	0.01
Fe_2O_3	2.96	12.46
K_2O	0.75	0.38
MgO	0.11	0.15
MnO	0.04	0.06
Na_2O	0.61	1.92
P_2O_5	0.04	0.02
SiO_2	84.17	66.09
TiO_2	0.17	0.14
L.O.I.*	7.52	8.82

* Loss on ignition.

The values of the defluoridation parameters for optimum fluoride removal are summarized in Table 7.

Adsorption isotherms

Adsorption isotherm is an equilibrium test providing a general idea of the effectiveness of the adsorbent in removing fluoride ions from water and also the maximum amount of fluoride ions that could be removed.[28]

In order to determine the adsorption capacity of Al/Fe oxide-modified DE for fluoride, and the nature of the adsorbent surface, sorption data were analysed to fit Langmuir and Freundlich isotherms. Langmuir model is an analytical equation that assumes monolayer coverage of adsorbent surface with adsorbate. Hence, Langmuir model is valid for monolayer adsorption onto a sorbent surface.[29]

Langmuir isotherm is given as

$$q_e = \frac{q_m K_L C_e}{1 + K_L C_e} \tag{10}$$

where q_e (mg/g) is the adsorption capacity, q_m (mg/g) is q_e for a complete monolayer, C_e (mg/L) is the equilibrium concentration and K_L (L/mg) is the adsorption equilibrium constant.

The linearised Langmuir equation (Eq. 11), known as Langmuir-1,[30] is the most commonly used linear forms of Langmuir equations

$$\frac{C_e}{q_e} = \frac{1}{q_m} C_e + \frac{1}{K_L q_m}. \tag{11}$$

The plot of C_e/q_e values against C_e for the sorption data at 297, 317 and 329 K gave straight lines with high correlation coefficients as shown in Figure 11; an indication of good fit of data

Table 7. Optimum defluoridation condition values.

Defluoridation condition	Value at optimum fluoride removal
Contact time (min)	50
Sorbent dosage (g)	0.6
Adsorbate concentration (mg/L)	10
Equilibrium pH	6.70

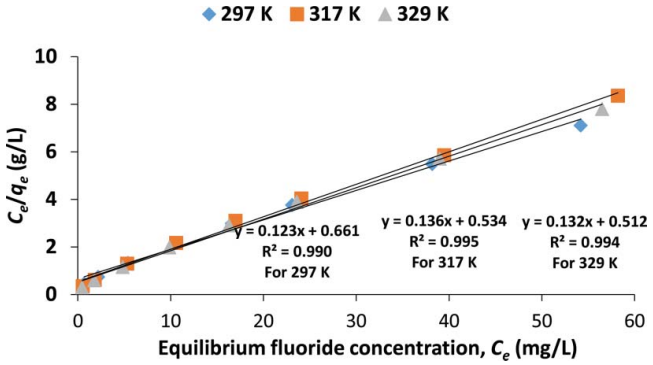

Figure 11. Langmuir isotherm plots at 297, 317 and 329 K (contact time: 50 min, initial fluoride concentrations: 10, 20, 30, 40, 50, 60, 80 and 100 mg/L, volume of solution: 100 mL, adsorbent dosage: 0.6 g and shaking speed: 200 rpm).

to the Langmuir isotherm. Hence, there was possibly a monolayer adsorption of fluoride on the smooth surface of the adsorbent.

Freundlich model is an empirical equation that takes into consideration the heterogeneity of the sorbent surface.[31]

The isotherm is given as

$$q_e = K_F C_e^{1/n}. \tag{12}$$

The linear form is represented by the following equation:

$$\log q_e = \log K_F + \frac{1}{n} \log C_e. \tag{13}$$

K_F and n are the Freundlich constants whose values depend on experimental conditions. K_F represents the adsorption capacity based on Freundlich isotherm while $1/n$ is the heterogeneity factor. Where $1/n$ values are much less than 1, the adsorbents are heterogeneous.[32] The values of K_F and $1/n$ can be computed from the plots of log q_e versus log C_e.

The plot oflog q_e against log C_e for the sorption data at 297, 317 and 329 K gave straight lines with high correlation coefficients as shown in Figure 12. The correlation coefficients are however less than those of Langmuir isotherm at each temperature. Therefore Langmuir isotherm gave better fits to the sorption data. The minimum adsorption capacities, K_F calculated at the evaluated temperatures as shown in Table 8 are higher

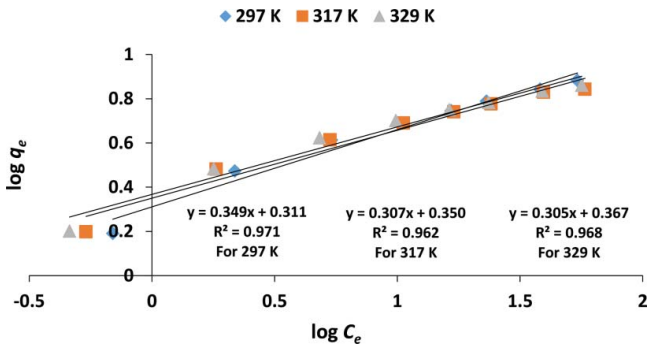

Figure 12. Freundlich isotherm plots at 297, 317 and 329 K (initial fluoride concentrations: 10, 20, 30, 40, 50, 60, 80 and 100 mg/L, volume of solution: 100 mL, adsorbent dosage: 0.6 g, shaking speed: 200 rpm).

Table 8. Calculated Langmuir and Freundlich isotherm parameters.

	Langmuir isotherm constants			Freundlich isotherm constants R^2		
Temperature (K)	q_m (mg/g)	K_L (L/mg)	R^2	$1/n$	K_F	R^2
297	8.1301	0.1861	0.990	0.349	2.0464	0.971
317	7.3529	0.2547	0.995	0.307	2.2387	0.962
329	7.5758	0.2578	0.994	0.305	2.3281	0.968

than those obtained from the experiment. However, the heterogeneity of the adsorbent surface is established by the low values of the parameter $1/n$ (Table 8). The fitness of data to the two isotherms, consistently, at the three different evaluated temperatures is proof of applicability of the isotherms in describing the adsorption at the various fluoride concentrations.

Adsorption thermodynamics

Temperature influences the spontaneity of a chemical process among other driving forces. However, the spontaneity of a chemical reaction is wholly determined by a thermodynamic quantity defined as the Gibbs free energy change, ΔG^0.[33] The Gibbs free energy is given as

$$\Delta G^0 = \Delta H^0 - T\Delta S^0. \tag{14}$$

ΔH^0 is the standard enthalpy change while ΔS^0 is the entropy change. For a spontaneous sorption process, ΔG^0 must have a negative value.

In sorption equilibria, the equilibrium constant K_L which is the Langmuir's constant is related to the Gibbs free energy change by the following equation:

$$\Delta G^0 = -RT \ln K_L. \tag{15}$$

ΔG^0 is the standard Gibbs free energy change and R is the molar gas constant, 8.314 J mol^{-1} K^{-1}

$$\ln K_L = -\frac{\Delta H^0}{RT} + \frac{\Delta S^0}{R}. \tag{16}$$

ΔH^0 is known as the standard enthalpy change.

The linear form

$$\ln K_L = -\frac{\Delta H^0}{RT} + \text{constant} \tag{17}$$

is suitable for graphical determination of the standard enthalpy change from the slope of the linear plot of ln K_L against $1/T$.

The Gibbs free energy change calculated for the sorption data at the evaluated temperatures have negative values as shown in Table 9. This confirms the spontaneity of the sorption process at those temperatures.

The standard enthalpy change for the sorption of fluoride onto Al/Fe oxide-modified DE was obtained from the slope of the linear plot of ln K_L against $1/T$ (Fig. 13).
The slope of the linear plot is −1055.1.
Therefore from calculation, $\Delta H^0 = 8771.27$ J/mol.
The positive value of the standard enthalpy change is an indication that the fluoride sorption process is endothermic.

Adsorption kinetics

Two kinetic models for predicting the order of sorption process were evaluated. The Lagergren pseudo-first-order model is given as

$$\frac{dq_t}{dt} = k_1(q_e - q_t). \tag{18}$$

q_t (mg/g) is the fluoride concentration at any time t, q_e (mg/g) is the maximum sorption capacity of the pseudo-first-order and k_1 (min^{-1}) is the pseudo-first-order rate constant.
On integration Eq. 18 becomes

$$\log(q_e - q_t) = -\frac{k_1}{2.303}t + \log q_e. \tag{19}$$

The pseudo-first-order model was tested by fitting it to the adsorption data. However, the plots of log $(q_e - q_t)$ values against t did not give straight lines (Figure not given). Hence, the model was not applicable to the sorption process.

The pseudo-second-order model was also tested to see its applicability to the data. The model is presented in the following equation:

$$\frac{dq_t}{dt} = k_2(q_e - q_t)^2. \tag{20}$$

q_t (mg/g) is the fluoride concentration at any time t, q_e (mg/g) is the maximum sorption capacity of the pseudo-second-order and k_2 [g/(mg min)] is the rate constant for the pseudo-second-order process.

On integration, the following equation gives the linear form of the pseudo-second-order:

$$\frac{t}{q_t} = \frac{1}{k_2 q_e^2} + \frac{t}{q_e}. \tag{21}$$

Table 9. Adsorption thermodynamic parameters.

T (K)	$1/T$ (1/K)×10^3	ln K_L	K_L (L/kg)	ΔG^0 (J/mol)
297	3.367	5.2263	186.1	−12 905.04
317	3.155	5.5401	254.7	−14 601.11
329	3.040	5.5522	257.8	−15 186.92

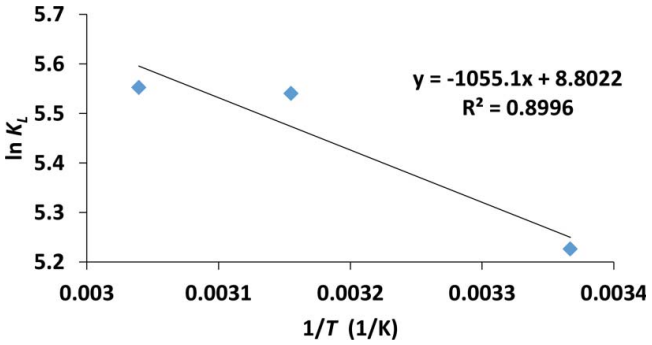

Figure 13. ln K_L as a function of reciprocal of adsorption temperatures.

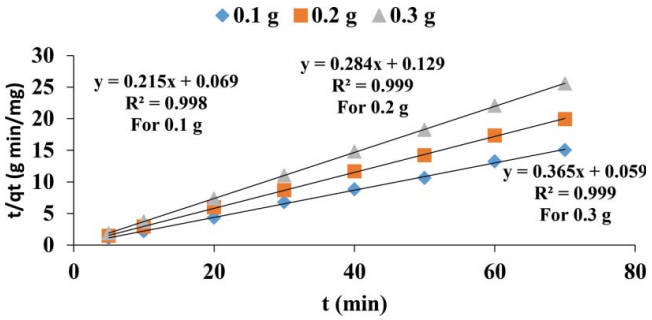

Figure 14. Pseudo-second-order profile at different adsorbent dosages (initial fluoride concentration: 10 mg/L, volume of solution: 100 mL, temperature: 297 K and shaking speed: 200 rpm).

The plot of $^{t}/_{q_t}$ values against time t for adsorbent dosages of 0.1, 0.2 and 0.3 g gave near perfect straight lines as shown in Figure 14. Hence, the data conformed to a pseudo-second-order; an indication of adsorption by chemisorption.

The calculated q_e and the experimental q_e were compared. The closeness of the two values as shown in Table 10 is an indication that the pseudo-second-order model was the appropriate kinetic model for the fluoride sorption.

Adsorption mechanisms

Intra-particle diffusion

The probable mechanism controlling the sorption rate was evaluated using the intra-particle diffusion model by Weber and Morris,[34] stated as

$$q_t = k_{id}\sqrt{t} + I \tag{22}$$

where k_{id} [mg/(g min$^{1/2}$)] is the intra-particle diffusion rate constant and I (mg/g) is a constant that has to do with the thickness of the boundary layer. Intra-particle diffusion could possibly be the rate-controlling step. If the plot of q_t against $\sqrt{t}$ is linear, then, intra-particle diffusion would be the rate controlling factor. This was however not the case when the intra-particle diffusion was evaluated in this study. That intra-particle diffusion could possibly not be the sorption rate determinant because of the much smaller size of fluoride ion to the pores of the sorbent. The ionic radius of fluoride is 1.33 Å.[35] The minimum pore diameter of the adsorbent as determined by BET analysis was 20.112 Å. There would therefore be no inhibition to fluoride ion movement through the adsorbent.

External diffusion

The external diffusion model by Lee et al.[36] was used to evaluate the possibility of external diffusion being the rate controlling step. The diffusion model is given as

$$\ln\frac{C_t}{C_0} = -k_f\frac{A}{V}t \tag{23}$$

where C_0 is the initial fluoride concentration, C_t is the concentration at time t, A/V is the external adsorption area to the total solution volume, t is the adsorption time, and k_f is the external diffusion coefficient. If a straight line is obtained from the plot of $\ln\frac{C_t}{C_0}$ against t, then external diffusion controls the sorption process.[36] The external diffusion plots for the sorption data were not linear and so external diffusion could not be the sorption rate limiting step.

The probable mechanism controlling the rate of fluoride sorption onto the adsorbent is either the electrostatic attraction of fluoride ions to the positively charged sorbent surface or the ion-exchange at the surface.[37,38]

Effect of co-existing anions

In groundwater water, there could be other anions along with fluoride which might possibly compete with fluoride for adsorption. Some of the common anions reported to compete with fluoride include NO_3^-, CO_3^{2-}, SO_4^{2-} and PO_4^{3-} ions.[39] The effect of each anion on fluoride adsorption was studied separately. The simulated groundwater was prepared by measuring 1 mL of 1,000 mg/L fluoride and 50 mL of 10 mg/L of the anion being evaluated into 100 mL volumetric flask. Milli-Q water was then added to the flask until the volume of solution was at the etched mark. The resulting solution which contained 10 mg/L fluoride and 5 mg/L anion was shaken and then transferred quantitatively into a 250-mL plastic bottle. A mass of 0.6 g of adsorbent was weighed into the flask and shaken for 50 min at 200 rpm. After equilibration, mixtures were centrifuged to remove the solid. The fluoride in supernatants was analysed using ORION fluoride ion-selective electrode. The effect of each anion on fluoride removal was

Table 10. Pseudo-second-order parameters at different adsorbent dosages.

Adsorbent dosage (g)	Equation	Experimental q_e(mg/g)	Calculated q_e (mg/g)	k_2 (L mg^{-1} min^{-1})
0.1	$y = 0.215x + 0.069$	4.651	4.720	0.6699
0.2	$y = 0.284x + 0.129$	3.521	3.520	0.6252
0.3	$y = 0.365x + 0.059$	2.740	2.743	2.2581

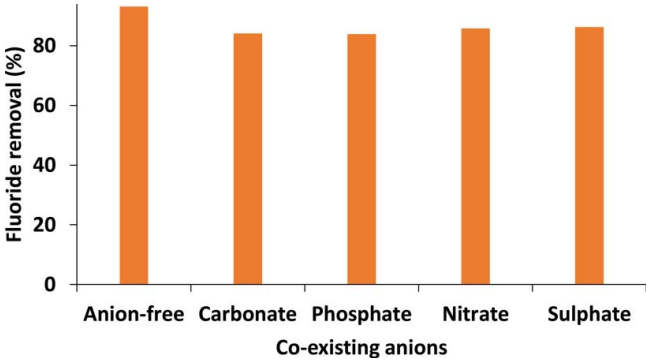

Figure 15. Effect of co-existing anions on fluoride removal (initial fluoride concentration: 10 mg/L, volume of solution: 100 mL, concentration of anion: 5 mg/L, adsorbent dosage: 0.6 g, contact time: 50 min, shaking speed: 200 rpm and temperature: 297 K).

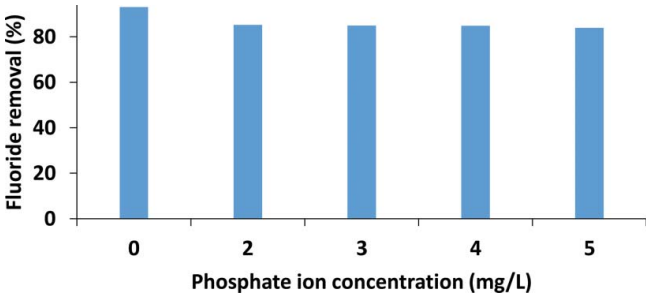

Figure 16. Dependence of percent fluoride removal on the concentration of co-existing phosphate ions (initial fluoride concentration: 10 mg/L, volume of solution: 100 mL, adsorbent dosage: 0.6 g, contact time: 50 min, shaking speed: 200 rpm and temperature: 297 K).

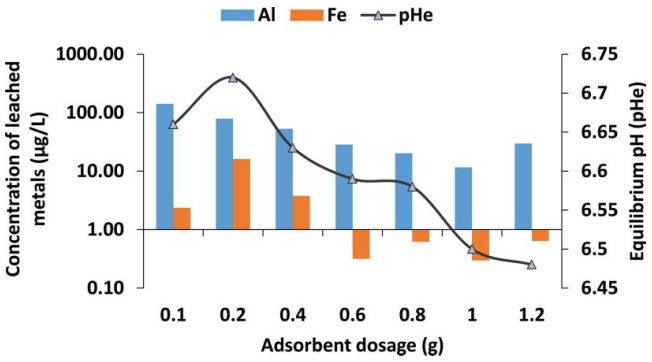

Figure 17. Concentration of leached metals as a function of adsorbent dosage (initial F^- concentration: 11.25 mg/L, volume of solution: 100 mL, contact time: 50 min, temperature: 297 K and shaking speed: 200 rpm).

Table 11. Concentrations of competing anions before and after defluoridation.

Co-existing anion	Initial concentration (mg/L)	Final concentration (mg/L)
Cl^-	31.6	40.9
Br^-	2.08	ND
NO_3^-	1.13	ND
SO_4^-	11.9	ND
PO_4^{3-}	ND	ND

ND: not detected.

determined based on the percent fluoride removal with the anion co-existing in water. This varied with the type of anion. Figure 15 shows the percent fluoride removal relative to the competing anion in water. The order in which the anions competed with fluoride is $SO_4^{2-} < NO_3^- < CO_3^{2-} \approx PO_4^{3-}$. There was no significant difference between CO_3^{2-} and PO_4^{3-} in competition with fluoride.

Negatively charged ions are naturally attracted to positively charged ones. The extent of attraction is dependent on the magnitude of charge and size of ion. Usually anions with higher charge magnitude are more strongly attracted to cations for bond formation than the univalent anions. This would probably explain why PO_4^{3-} competed most with F- for adsorption than any other anion. Equilibrium pH ranged between 6.80 and 6.98.

Further studies were carried out to determine the extent to which the concentration of phosphate could affect fluoride removal. The concentrations of phosphate considered along with 5 mg/L included 2, 3 and 4 mg/L. From the results, a concentration as low as 2 mg/L phosphate in water containing 10 mg/L fluoride could lower the percent fluoride removal by about 8%. Increasing the phosphate concentration within the range of 2–5 mg/L did not cause any significant change in percent fluoride removal above the value for 2 mg/L PO_4^{3-}. The trend is presented in Figure 16.

Correlation between leached metals and adsorbent dosage

The likelihood of aluminium and iron leaching into water at high adsorbent dosage was evaluated by analysing the supernatants obtained from the batch experiment involving different adsorbent dosages. The metal species were determined using ICP-MS analysis. The results are presented in Figure 17. The concentrations of Al and Fe species were in trace levels and so not of health concern.[1] The average equilibrium pH of solution was 6.59 ± 0.09.

Defluoridation of field water

The performance of Al/Fe oxide-modified DE in groundwater defluoridation was evaluated by batch technique. A dosage of 0.6 g of the sorbent was contacted with 100 mL of groundwater containing initially 5.53 mg/L fluoride and the mixture shaken for 50 min at 200 rpm. The initial and equilibrium pH of mixture were 6.92 and 6.80 respectively.

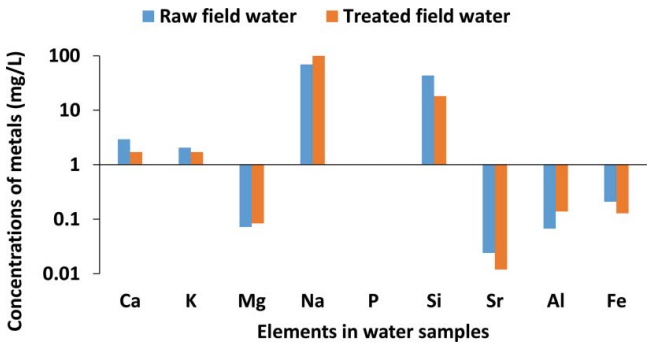

Figure 18. Concentrations of elements in field water in mg/L.

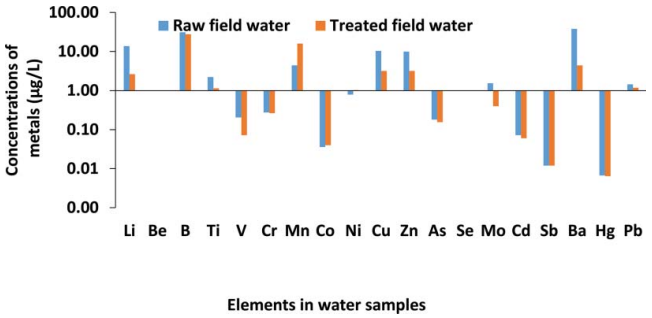

Figure 19. Concentrations of elements in treated field water in μg/L (volume of water: 100 mL, adsorbent dosage: 0.6 g, contact time: 50 min, shaking speed: 200 rpm).

After equilibration, the mixture was centrifuged and the supernatant analyzed for fluoride. The concentration of fluoride in the treated water was reduced from 5.53 to 0.928 mg/L. Hence, the percent fluoride removal was 83.2%. The anions in the original and treated groundwater were analyzed using Metrohm 850 Professional IC. The results of analysis are presented in Table 11.

Table 11 shows that the adsorbent removed all the competing anions except chloride below the detection limit of the IC instrument. The increase in the concentration of chloride in the treated water was a result of the leaching of chloride from the adsorbent. The source could be HCl used in the treatment of the raw DE.

The full chemical analysis of the field water before and after defluoridation was done using ICP-MS. From the results presented in Figures 18 and 19, the concentrations of all the elements evaluated in the raw and treated field water were below the WHO Guidelines for Drinking-water Quality.[1] Hence, the treated water might be safe for consumption.

Conclusion

Al/Fe oxide-modified DE has a high fluoride removal potential. The optimum adsorption capacity was 7.633 mg/g for 100 mg/L F^- at 297 K. The maximum percent F- removal was 93.1% at solid-liquid ratio of 0.6 g/100 mL (initial fluoride concentration: 10 mg/L, contact time: 60 min, temperature: 297 K, and shaking speed: 200 rpm). Contact time and temperature change had no significant effect on fluoride removal. At 5 mg/L co-existing anion concentration, reduction in percent F- removal was at most 9.2% for PO_4^{3-}. A sorbent dosage of 0.6 g/100 mL reduced fluoride in field water from 5.53 to 0.928 mg/L, a value below the WHO guideline of 1.5 mg/L for fluoride in drinking water. Hence, with the water treatment, the chances of consumers having fluorosis are much reduced.

Conformance of data to Langmuir and Freundlich isotherms confirmed both monolayer and multi-site adsorption of F- onto the adsorbent surface. Data fitted better into the Langmuir isotherm than Freundlich isotherm. Sorption kinetics was better modelled using the pseudo-second-order model. Hence, adsorption was by chemisorption. The adsorption rate limiting step was most probably the process involving ion-exchange or attraction of F- to the sorbent surface as neither intra-particle nor external diffusions was the rate limiting mechanism.

Funding

This work was supported by WRC Project No. K5/2363/3, NRF Project No. CSUR13092849176, Grant No. 90288, THRIP Project No. TP12082610644 and Directorate of Research & Innovation, University of Venda.

References

[1] World Health Organization (WHO). Chemical fact sheets. *Guidelines for Drinking-water Quality*; 4th Ed.; Gutenberg: Malta, 2011; 370–373.
[2] Battaleb-Looie, S.; Moore, F. A study of fluoride occurrence in Posht-e-Kooh-e-Dashtestan, South of Iran. World Appl. Sci. J. **2010**, *8*(11), 1317–1321.
[3] Hammer, M.J. Need for fluoridation of desalinated water supplies. Aqua **1986**, *4*, 179–182.
[4] World Health Organization (WHO). Background document for development of WHO Guidelines for Drinking-water Quality. *Fluoride in drinking-water*. WHO/SDE/WSH/03.04/96, 2004; 5–7.
[5] Adihikary, S.K.; Tipnis, U.K.; Harkare, W.P.; Govinda, K.P. Defluoridation during desalination of brackish water by electrodialysis. Desalination **1989**, *71*, 301–312.
[6] Simons, R. Trace element removal from ash dam waters by nanofiltration and diffusion dialysis, Desalination. **1993**, *89*, 325–341.
[7] Karthikeyan, G.; Pius, A.; Alagumuthu, G. Fluoride adsorption studies of montmorillonite clay. Indian J. Chem. Technol. **2005**, *12*, 263–272.
[8] Janardhana, C.; Rao, G.N.; Sathish, R.S.; Lakshman, V.S. Study on defluoridation of drinking water by impregnation of metal ions in activated charcoal. Indian J. Chem. Technol. **2006**, *13*, 414–416.
[9] Ghorai, S.; Pant, K.K. Equilibrium, kinetics and breakthrough studies for adsorption of fluoride on activated alumina. Sep. Purif. Technol. **2005**, *42*, 265–271.
[10] Bjorvatn, K.; Bardsen, A.; Tekle-Haimanot, R. Defluoridation of drinking water by use of clay/soil. In *Defluoridation; Laboratory Experiences*, Proceedings of the 2nd International Workshop on Fluorosis Prevention and Defluoridation of Water, Nazareth, Ethiopia, Nov 19–25, 1997; Dahi, E., Nielsen, J.M., Eds.; The International Society for Fluoride Research: New Zealand, 1997; 100–105.
[11] Gitari, W.M.; Ngulube, T.; Masindi, V.; Gumbo, J.R. Defluoridation of groundwater using Fe^{3+}-modified bentonite clay: optimization of adsorption conditions. Desal. Water Treat. **2013**, *53*(6), 1578–1591.
[12] Barathi, M.; Kumar, A.S.K.; Rajesh, N. Aluminium hydroxide impregnated macroreticular aromatic polymeric resin as a sustainable option for defluoridation. J. Environ. Chem. Eng. **2015**, *3*, 630–641.
[13] Khraisheh, M.A.M.; Al-Degs, Y.S.; Mcminn, W.A.M. Remediation of wastewater containing heavy metals using raw and modified diatomite. Chem. Eng. J. **2004**, *99*, 177–184.
[14] Khraisheh, M.A.M.; Al-Ghouti, M.A.; Allen, S.J.; Ahmad, M.N.M. The effect of pH, temperature and molecular size on the removal of dyes from textile effluent using manganese oxides modified diatomite. Water Environ. Res. **2004**, *76*, 2655–2663.
[15] Ibrahim, S.S.; Selim, A.Q. Heat treatment of natural diatomite. Physicochem. Probl. Miner. Process **2012**, *48*(2), 413–424.
[16] Datsko, T.Ya.; Zelentsov, V.I.; Dvornikova, E.E. Physicochemical and adsorption-structural properties of diatomite modified with aluminum compounds. Surface Eng. Appl. Electrochem. **2011**, *47*(6), 530–539.
[17] Yao, R.; Meng, F.; Zhang, L.; Ma, D.; Wang, M. Defluoridation of water using neodymium-modified chitosan. J. Hazard. Mater. **2009**, *165*, 454–460.
[18] Shimelis, B.; Zewge, F.; Chandravanshi, B.S. Removal of excess fluoride from water by aluminum hydroxide. Bull. Chem. Soc. Ethiop. **2006**, *20*(1), 17–34.
[19] Meenakshi, S.; Sundaram, C.S.; Sukumar, R. Enhanced fluoride sorption by mechanochemically activated kaolinites. J. Hazard. Mater. **2008**, *153*, 164–172.

[20] Wambu, E.W.; Onindo, C.O.; Ambusso, W.J.; Muthakia, G.K. Fluoride adsorption onto acid-treated diatomaceous mineral from Kenya. Mater. Sci. Appl. **2011**, *2*, 1654–1660.
[21] Sakhare, N.; Lunge, S.; Rayalu, S.; Bakardjiva, S.; Subrt, J.; Devotta, S.; Labhsetwar, N. Defluoridation of water using calcium aluminate material. Chem. Eng. J. **2012**, 406–414.
[22] Kagne, S.; Jagtap, S.; Thakare, D.; Devotta, S.; Rayalu, S.S. Bleaching powder: a versatile adsorbent for the removal of fluoride from aqueous solution. Desalination **2009**, *243*, 22–31.
[23] Tripathy, S.S.; Bersillon, J-L.; Gopal, K. Removal of fluoride from drinking water by adsorption onto alum-impregnated activated alumina. Sep. Purif. Technol. **2006**, *50*, 310–317.
[24] Nasr, A.B.; Walha, K.; Charcosset, C.; Amar, R.B. Removal of fluoride ions using cuttlefish bones. J. Fluorine Chem. **2011**, *132*, 57–62.
[25] Gavriloaiei, T.; Gavriloaiei, D-I. Determination of surface charge for metal oxides. Anal. St. Univ. "Al. I. Cuza" Geologie **2008**, *54*, 11–18.
[26] Bishop, P.L.; Sancoucy, G. Fluoride removal from drinking water by fluidized activated alumina adsorption. J. AWWA **1978**, *70*, 554–559.
[27] Shrivastava, B.K.; Vani, A. Comparative study of defluoridation technologies in India. Asian J. Exp. Sci. **2009**, *23*(1), 269–274.
[28] Tembhurkar, A.R.; Dongre, S. Studies on fluoride removal using adsorption process. J. Environ. Sci. Eng. **2006**, *48*(3), 151–156.
[29] Langmuir, I. The adsorption of gases on plane surfaces of glass, mica and platinum. J. Am. Chem. Soc. **1918**, *40*, 1361–1403.
[30] Kinniburgh, D.G. General purpose adsorption isotherms. Environ. Sci. Technol. **1986**, *20*(9), 895–904.
[31] Freundlich, H.M.F. Over the adsorption in solution. J. Phys. Chem. **1906**, *57*, 370–485.
[32] Papageorgiou, K.S.; Katsaros, K.F.; Kouvelos, P.E.; Nolan, W.J.; LeDeit, H.; Kanellopoulos, K.N. Heavy metal sorption by calcium alginate beads from *Laminaria digitata*. J. Hazard. Mater. **2006**, *137*, 1765–1772.
[33] Jenkins, H.D.B. *Chemical Thermodynamics at a Glance*; Blackwell Publishing Ltd.: Oxford, 2008; 136–137.
[34] Weber, W.J.; Morris, J.C. Kinetics of adsorption on carbon from solution. J. Sanit. Eng. Div./Am. Soc. Civ. Eng. **1963**, *89*, 31–60.
[35] Ruben, S. *Handbook of the Elements*; Open Court Publishing Company: La Salle, IL, 1985; 30.
[36] Lee, C.K.; Low, K.S.; Chew, S.L. Removal of anion dyes by water hyacinth roots. Adv. Environ. Res. **1999**, *3*, 343–351.
[37] Weber, W.J.; DiGiano, F.A. Process dynamics in environmental systems. *Environmental Science and Technology Series*; Wiley & Sons: New York, 1996; 89–94.
[38] Gulipalli, C.H.S.; Prasad, B.; Wasewar, K.L. Batch study, equilibrium and kinetics of adsorption of selenium using rice husk ash (RHA). J. Eng. Sci. Technol. **2011**, *6*(5), 586–605.
[39] Chen, N.; Zhang, Z.; Feng, C.; Zhu, D.; Yang, Y.; Sugiura, N. Preparation and characterization of porous granular ceramic containing dispersed aluminium and iron oxides as adsorbents for fluoride removal from aqueous solution. J. Hazard. Mater. **2011**, *186*, 863–868.